METALLURGICAL TECHNOLOGIES / МЕТАЛЛУРГИЧЕСКИЕ ТЕХНОЛОГИИ

UDC 536.425:539.25:539.351
DOI 10.17073/0368-0797-2025-1-30-39

Original article
Оригинальная статья

Influence of inclined electric field on decay of a liquid jet during heat treatment and surfacing

S. A. Nevskii ✉, L. P. Bashchenko, V. D. Sarychev, A. Yu. Granovskii, D. V. Shamsutdinova

Siberian State Industrial University (42 Kirova Str., Novokuznetsk, Kemerovo Region – Kuzbass 654007, Russian Federation)

✉ nevskiy.sergei@yandex.ru

Abstract. The combined effect of inclined electric fields and a transverse acoustic field on the Kelvin–Helmholtz instability of the interface of viscous electrically conductive liquids is studied using the example of air – water and argon – iron systems. An inclined electric field, regardless of the effect of sound vibrations, leads to the increased Kelvin–Helmholtz instability in the micrometer wavelength range. The most intense increase in the disturbances of the interface is observed at the angle of inclination of the electric field $\pi/3$. This opens up new opportunities for the development of technologies for accelerated cooling of rolled products and surfacing materials by regulating the drop transfer of material. The combined effect of acoustic and electric fields has an ambiguous effect on the Kelvin–Helmholtz instability. In the case of an air – water system, sound vibrations lead to suppression of the Kelvin–Helmholtz instability, while a tangential electric field with a strength of $3 \cdot 10^6$ V/m enhances this effect, and a normal field, on the contrary, weakens it. For the argon – iron system, sound vibrations lead to the complete disappearance of the viscosity-conditioned maximum and to a significant decrease in the growth rate of disturbances at the interface, which corresponds to the first maximum. Application of a horizontal electric field with a strength of $3 \cdot 10^7$ V/m significantly weakens the effect of suppressing the Kelvin–Helmholtz instability, while in a vertical field, on the contrary, increases it. It was established that the restoration of the first hydrodynamic maximum in a normal electric field is possible with a ratio of specific electrical conductivities σ greater than 0.012, regardless of the presence of a sound field. A change in the influence of the vertical electric field from a stabilizing to a destabilizing one is possible with a ratio of σ from 0.015 or more.

Keywords: electric field, acoustic field, heat treatment, air–water system, argon–iron system, Kelvin–Helmholtz instability, viscous potential approximation

Acknowledgements: The work was supported by the Russian Science Foundation (grant No. 22-79-10229, https://rscf.ru/project/22-79-10229/).

For citation: Nevskii S.A., Bashchenko L.P., Sarychev V.D., Granovskii A.Yu., Shamsutdinova D.V. Influence of inclined electric field on decay of a liquid jet during heat treatment and surfacing. *Izvestiya. Ferrous Metallurgy*. 2025;68(1):30–39. https://doi.org/10.17073/0368-0797-2025-1-30-39

Влияние наклонного электрического поля на распад струи жидкости в процессах термообработки и наплавки

С. А. Невский ✉, Л. П. Бащенко, В. Д. Сарычев, А. Ю. Грановский, Д. В. Шамсутдинова

Сибирский государственный индустриальный университет (Россия, 654007, Кемеровская обл. – Кузбасс, Новокузнецк, ул. Кирова, 42)

✉ nevskiy.sergei@yandex.ru

Аннотация. Изучено совместное воздействие наклонных электрических полей и поперечного акустического поля на неустойчивость Кельвина–Гельмгольца границы раздела вязких электропроводных жидкостей на примере систем воздух – вода и аргон – железо. Наклонное электрическое поле вне зависимости от воздействия звуковых колебаний приводит к усилению неустойчивости Кельвина–Гельмгольца в микрометровом диапазоне длин волн. Наиболее интенсивный рост возмущений поверхности раздела наблюдается при угле наклона электрического поля $\pi/3$. Это открывает новые возможности для разработки технологий ускоренного охлаждения проката и наплавки материалов путем регулирования капельного переноса материала. Совместное воздействие акустических и электрических полей оказывает неоднозначное влияние на неустойчивость Кельвина–Гельмгольца. В случае системы воздух – вода звуковые колебания приводят к подавлению неустойчивости Кельвина–Гельмгольца, при этом тангенциальное электрическое поле напряженностью $3 \cdot 10^6$ В/м усили-

вает данный эффект, а нормальное поле, наоборот, ослабляет его. Для системы аргон – железо звуковые колебания приводят к полному исчезновению вязкостно-обусловленного максимума и к значительному снижению скорости роста возмущений поверхности раздела, которая соответствует первому максимуму. Приложение горизонтального электрического поля напряженностью $3 \cdot 10^7$ В/м значительно ослабляет эффект подавления неустойчивости Кельвина–Гельмгольца, а в вертикальном поле он, наоборот, усиливается. Установлено, что восстановление первого гидродинамического максимума в нормальном электрическом поле возможно при соотношении удельных электрических проводимостей σ более 0,012 вне зависимости от наличия звукового поля. Смена знака влияния вертикального электрического поля со стабилизирующего на дестабилизирующее возможно при соотношении σ от 0,015 и более.

Ключевые слова: электрическое поле, акустическое поле, термообработка, система воздух – вода, система аргон – железо, неустойчивость Кельвина–Гельмгольца, вязко-потенциальное приближение

Благодарности: Исследование выполнено за счет гранта Российского научного фонда № 22-79-10229, https://rscf.ru/project/22-79-10229/.

Для цитирования: Невский С.А., Бащенко Л.П., Сарычев В.Д., Грановский А.Ю., Шамсутдинова Д.В. Влияние наклонного электрического поля на распад струи жидкости в процессах термообработки и наплавки. *Известия вузов. Черная металлургия*. 2025;68(1):30–39. https://doi.org/10.17073/0368-0797-2025-1-30-39

Introduction

The Kelvin–Helmholtz instability occurs in various research fields, ranging from terrestrial magnetohydrodynamics [1] and turbulent liquid mixing [2] to processes such as coating deposition by electrical explosion [3] and astrophysical phenomena like the solar wind [4]. This instability serves as a powerful trigger that disrupts the stability of systems involving the mixing of two or more liquids with different properties. Some of the most notable applications of this instability include acoustic modes in air-consuming systems such as boilers, jet engines, and gas turbines [5]. Another significant application of this instability is the breakup of a liquid jet into droplets in an electric field [6; 7]. This phenomenon underlies the operation of precision devices that are integral to various technological processes, such as electric arc welding and the production of ultrafine refractory powders [6; 7]. In [8], the influence of an inclined electric field on the Kelvin–Helmholtz instability of two ideal dielectric liquids was studied, revealing the conditions under which the liquid transitions to a stable mode under a horizontal electric field. It was also demonstrated that the vertical component of the electric field exerts a destabilizing effect. Another promising application of this instability is the accelerated cooling of rolled products. In [9], it was shown that by controlling the velocity of the air – water system, it is possible to achieve the formation of droplets in the nanometer range. Upon impacting rolled products, these droplets induce a thermoelastic wave, thereby increasing their impact toughness.

The origin and development of the Kelvin–Helmholtz instability of two viscous liquids were investigated in [10; 11]. A key feature of these studies is the use of the viscous potential approximation. This approach assumes the absence of shear stress components of the stress tensor at the interface, while the viscosity of the liquid is taken into account only in the condition of continuity of normal stresses at the interface [10]. In the general case, the situation is complicated by the need to determine the velocity profile of the fluid, and as shown in [11; 12], there is no analytical solution for the stability of a flow with a complex velocity profile. However, at high wavenumbers (short wavelengths), this approximation is justified, as demonstrated in [13].

The interaction of the Kelvin–Helmholtz instability with ultrasonic vibrations in the case of a problem with planar geometry under the viscous potential flow approximation was studied in [14; 15]. The interaction of the Kelvin–Helmholtz instability with ultrasonic vibrations in a planar geometry under the viscous potential approximation was studied in [14; 15]. It was assumed that the effect of acoustic vibrations is equivalent to an effective oscillating gravitational field. It was found that acoustic influence shifts the maximum growth rate toward higher wavenumbers [15], and a stability region was identified between weak acoustic excitation and parametric resonance.

The objective of this study was to investigate the combined influence of an inclined electric field and a transverse acoustic field on the stability of the planar surface of an electrically conductive liquid using the example of the iron – argon and air – water systems under the viscous potential flow approximation. The simultaneous application of these two factors enables the creation of micro- and nanodroplet flow patterns, which is crucial for the development of new technologies in welding, surfacing, and accelerated cooling of rolled products.

Problem statement

Consider the instability of the planar interface between two viscous electrically conductive fluids. The first fluid is characterized by density ρ_1, kinematic viscosity ν_1, electrical conductivity σ_1, and dielectric permittivity ε_1 (Fig. 1). It occupies the region ($-\infty \le x \le +\infty$ and $-h_1 \le z \le 0$) and moves with a horizontal velocity U_1. The second fluid occupies the region ($-\infty \le x \le +\infty$ and $0 \le z \le h_2$) and is characterized by density ρ_2, kinematic viscosity ν_2, electrical conductivity σ_2, and dielectric permittivity ε_2. The horizontal velocity of the second fluid

is U_2. The variable ξ represents the deviation of the interface from its equilibrium position (Fig. 1).

The flow velocities of the first and second fluids are much lower than the speed of sound; therefore, they can be considered incompressible. The kinematics of the interface motion is described by the function $F(x, z, t) = z - \xi(x, t)$. Thus $\vec{n} = \frac{\nabla F}{|\nabla F|} = \frac{-\frac{\partial \xi}{\partial x}\vec{e}_x + \vec{e}_z}{\sqrt{1+\left(\frac{\partial \xi}{\partial x}\right)^2}}$ the normal vector is defined as (where ∇ is the gradient operator. In the linear approximation, the normal vector $\vec{n} = -\frac{\partial \xi}{\partial x}\vec{e}_x + \vec{e}_z$ takes the form. The system under consideration is placed in an external transverse acoustic field and an inclined electric field relative to the planar interface of the fluid (Fig. 1). The electric field vector, taking into account the disturbances of the interface, is given by $\vec{E} = E_{0x}\vec{e}_x - E_{0z}\vec{e}_z - \nabla\psi$ (where ψ is the disturbance of the electric potential, and E_{0x} and E_{0z} are the normal and tangential components of the unperturbed electric field, respectively). The inclination angle of the electric field (Fig. 1) relative to the unperturbed surface β is defined as $\text{arctg}\left(\frac{E_{0z}}{E_{0x}}\right)$.

The fundamental linearized equations of the viscous potential flow model for relatively small disturbances, taking into account the electric field, according to [10; 15], are given as:

$$\begin{aligned} \Delta\Phi_1 = 0;\ -h_1 < z < 0; \\ \Delta\Phi_2 = 0;\ 0 < r < h_2; \\ \Delta\psi_1 = 0;\ -h_1 < z < 0; \\ \Delta\psi_2 = 0;\ 0 < r < h_2, \end{aligned} \tag{1}$$

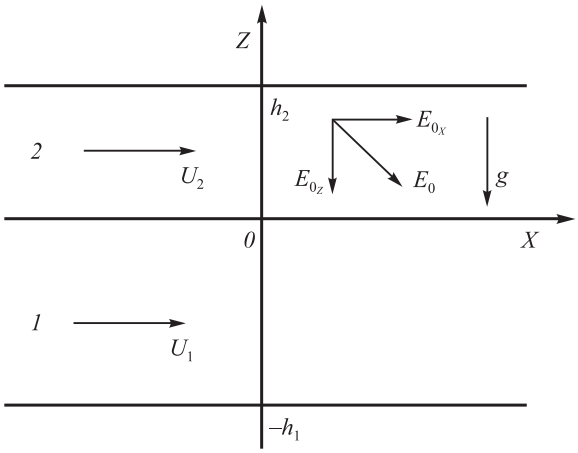

Fig. 1. On formulation of the problem of origin and development of the Kelvin–Helmholtz instability

Рис. 1. К постановке задачи о возникновении и развитии неустойчивости Кельвина–Гельмгольца

where Φ is represents the velocity potential disturbance.

When deriving the first and second equations of system (1), the terms associated with the electric field were neglected, which is valid for electrically conductive liquids [16 – 18], in the absence of a volumetric charge. Therefore, the electric field component will only be considered in the boundary conditions at the liquid – gas interface. At the boundaries h_2 and h_1, we impose conditions ensuring the absence of disturbances in the flow velocity and the electric field:

$$\begin{aligned} z = -h_1:\ \frac{\partial \Phi_1}{\partial z} = 0;\ \frac{\partial \psi_1}{\partial x} = 0; \\ z = h_2:\ \frac{\partial \Phi_2}{\partial z} = 0;\ \frac{\partial \psi_2}{\partial x} = 0. \end{aligned} \tag{2}$$

The boundary conditions for the disturbances of the flow potential of the liquid at the interface, taking into account the electric field, are given by:

$$\begin{aligned} z = 0:\ \frac{\partial \Phi_1}{\partial z} = \frac{\partial \xi}{\partial t} + U_1\frac{\partial \xi}{\partial z};\ \frac{\partial \Phi_2}{\partial z} = \frac{\partial \xi}{\partial t} + U_2\frac{\partial \xi}{\partial z}; \\ -p_1 + 2\rho_1\nu_1\frac{\partial^2 \Phi_1}{\partial z^2} + p_{s1} - \frac{1}{2}\varepsilon_1\varepsilon_0\left(E_{1n}^2 - E_{1\tau}^2\right) + \\ + p_2 - 2\rho_2\nu_2\frac{\partial^2 \Phi_2}{\partial z^2} - p_{s2} + \frac{1}{2}\varepsilon_2\varepsilon_0\left(E_{2n}^2 - E_{2\tau}^2\right) = \gamma\frac{\partial^2 \xi}{\partial x^2}, \end{aligned} \tag{3}$$

where U_i is the velocity of the i-th fluid; $p_i = -\rho_i \times \left(\frac{\partial \Phi_i}{\partial t} + U_i\frac{\partial \Phi_i}{\partial x}\right)$ is the pressure disturbance in the i-th fluid; p_{si} is the disturbance of the pressure of the acoustic field; $i = 1, 2$ is the fluid index; γ is the surface tension; E_{in} and $E_{i\tau}$ are the normal and tangential components of the field, respectively.

The boundary conditions for the electric field at the interface are defined as [19]:

$$\vec{n}\cdot\vec{E}_1 = \vec{n}\cdot\vec{E}_2;\ \sigma_1\left(\vec{n}\cdot\vec{E}_1\right) = \sigma_2\left(\vec{n}\cdot\vec{E}_2\right). \tag{4}$$

Substituting the above values of the normal vector and the electric field into equation (4) and subsequently linearizing, taking into account that at the interface of two conductors $\sigma_1 E_{01z} = \sigma_2 E_{02z}$, and $E_{01x} = E_{02x}$, leads to the following:

$$\begin{aligned} E_{10z}\frac{\partial \xi}{\partial x} + \frac{\partial \psi_1}{\partial x} = E_{20z}\frac{\partial \xi}{\partial x} + \frac{\partial \psi_2}{\partial x}; \\ \sigma_1\left(E_{10x}\frac{\partial \xi}{\partial x} + \frac{\partial \psi_1}{\partial z}\right) = \sigma_2\left(E_{20x}\frac{\partial \xi}{\partial x} + \frac{\partial \psi_2}{\partial z}\right). \end{aligned} \tag{5}$$

The solution to equations (1) will be sought in the form:

$$\begin{gathered}\Phi_1(x,z,t)=A_1\cosh\left[k(z+h_1)\right]\exp(\omega t+ikx);\\ \Phi_2(x,z,t)=A_2\cosh\left[k(z-h_2)\right]\exp(\omega t+ikx);\\ \psi_1(x,z,t)=A_3\sinh\left[k(z+h_1)\right]\exp(\omega t+ikx);\\ \psi_2(x,z,t)=A_4\sinh\left[k(z-h_2)\right]\exp(\omega t+ikx);\\ \xi(x,t)=\xi_0\exp(\omega t+ikx).\end{gathered}\tag{6}$$

Substituting the third, fourth, and fifth equations of (6) into equation (5) leads to the following system of equations for the constants A_3 and A_4:

$$\begin{gathered}A_3\sinh(kh_1)+A_4\sinh(kh_2)=\left(E_{20z}-E_{10z}\right)\xi_0;\\ A_3\sigma_1\cosh(kh_1)-A_4\sigma_2\cosh(kh_2)=\\ =i\xi_0\left(\sigma_2E_{20x}-\sigma_1E_{10x}\right).\end{gathered}\tag{7}$$

The solution to system (7) after transformation takes the form:

$$\begin{gathered}A_3=-\left\{\left[i\left(\sigma_1E_{10x}-\sigma_2E_{20x}\right)+\left(\sigma_2E_{10z}-\sigma_2E_{20z}\right)\times\right.\right.\\ \left.\left.\times\coth(kh_2)\right]\xi_0\right\}\times\\ \times\left\{\sinh(kh_1)\left[\coth(kh_1)\sigma_1+\coth(kh_2)\sigma_2\right]\right\}^{-1};\\ A_4=-\left\{\left[i\left(\sigma_1E_{10x}-\sigma_2E_{20x}\right)+\left(\sigma_1E_{20z}-\sigma_1E_{10z}\right)\times\right.\right.\\ \left.\left.\times\coth(kh_1)\right]\xi_0\right\}\times\\ \times\left\{\sinh(kh_2)\left[\coth(kh_1)\sigma_1+\coth(kh_2)\sigma_2\right]\right\}^{-1}.\end{gathered}\tag{8}$$

Then, the disturbances of the electric potential will take the following form:

$$\begin{gathered}\psi_1(x,z,t)=-\left\{\left[i(\sigma_1E_{10x}-\sigma_2E_{20x})+\right.\right.\\ \left.\left.+(\sigma_2E_{10z}-\sigma_2E_{20z})\coth(kh_2)\right]\sinh\left[k(z+h_1)\right]/\right.\\ \left./\left\{\sinh(kh_1)\left[\coth(kh_1)\sigma_1+\coth(kh_2)\sigma_2\right]\right\};\right.\\ \xi_0\exp(\omega t+ikx);\\ \psi_2(x,z,t)=\left\{\left[i(\sigma_1E_{10x}-\sigma_2E_{20x})+\right.\right.\\ \left.\left.+(\sigma_1E_{20z}-\sigma_1E_{10z})\coth(kh_1)\right]\sinh\left[k(z-h_2)\right]/\right.\\ \left./\left\{\sinh(kh_2)\left[\coth(kh_1)\sigma_1+\coth(kh_2)\sigma_2\right]\right\};\right.\\ \xi_0\exp(\omega t-ikx).\end{gathered}\tag{9}$$

To derive the disturbances of the flow potential, we substitute the first, second, and fifth equations of system (6) into the kinematic boundary conditions (3). As a result, we obtain:

$$\begin{gathered}\Phi_1(x,z,t)=\frac{\omega+ikU_1}{k\sinh(kh_1)}\times\\ \times\cosh\left[k(z+h_1)\right]\xi_0\exp(\omega t+ikx);\\ \Phi_2(x,z,t)=-\frac{\omega+ikU_2}{k\sinh(kh_2)}\times\\ \times\cosh\left[k(z-h_2)\right]\xi_0\exp(\omega t+ikx).\end{gathered}\tag{10}$$

The contribution of the acoustic field to the pressure is determined in the same way as in [14; 15]: $p_{si}=\rho_i g_{eff}\xi_0\times$ $\times\exp(\omega t+ikx)$ (where $g_{eff}=g-\Omega U_a\cos(\Omega t)$ is the effective acceleration; Ω and U_a are the frequency and amplitude of the acoustic excitation. Substituting (9) and (10) into the dynamic boundary condition (3) and performing subsequent transformations, taking into account that at $z=0$: $\sigma_1E_{01z}=\sigma_2E_{02z}$, $E_{01x}=E_{02x}$, leads to the following dispersion equation:

$$\begin{gathered}a_0\omega^2+2(a_1+ib_1)\omega+a_2+ib_2=0;\\ a_0=\rho_1\coth(kh_1)+\rho_2\coth(kh_2);\\ a_1=\rho_1\nu_1k^2\coth(kh_1)+\rho_2\nu_2k^2\coth(kh_2);\\ b_1=\rho_1U_1k\coth(kh_1)+\rho_2U_2k\coth(kh_2);\\ a_2=-k^2\left[\rho_1U_1^2\coth(kh_1)+\rho_2U_2^2\coth(kh_2)\right]+\\ +\gamma k^3+(\rho_1-\rho_2)g_{eff}k+\\ +\varepsilon_1\varepsilon_0k^2\left[\frac{(\sigma_1-\sigma_2)E_{20x}^2}{\coth(kh_1)\sigma_1+\coth(kh_2)\sigma_2}-\right.\\ \left.-\frac{\sigma_2^2(\sigma_1-\sigma_2)\coth(kh_1)\coth(kh_2)E_{20z}^2}{\sigma_1^2\left[\coth(kh_1)\sigma_1+\coth(kh_2)\sigma_2\right]}\right]+\\ +\varepsilon_2\varepsilon_0k^2\left[\frac{(\sigma_1-\sigma_2)\coth(kh_1)\coth(kh_2)E_{20z}^2}{\coth(kh_1)\sigma_1+\coth(kh_2)\sigma_2}-\right.\\ \left.-\frac{(\sigma_1-\sigma_2)E_{20x}^2}{\coth(kh_1)\sigma_1+\coth(kh_2)\sigma_2}\right];\\ b_2=\left\{\varepsilon_1\varepsilon_0k^2\sigma_2(\sigma_1-\sigma_2)\left[\coth(kh_1)+\coth(kh_2)\right]\times\right.\\ \left.\times E_{20x}E_{20z}\right\}/\left\{\sigma_1\left[\coth(kh_1)\sigma_1+\coth(kh_2)\sigma_2\right]\right\}+\\ +\left\{\varepsilon_2\varepsilon_0k^2(\sigma_1-\sigma_2)\left[\coth(kh_1)+\coth(kh_2)\right]\times\right.\\ \left.\times E_{20x}E_{20z}\right\}/\left\{\coth(kh_1)\sigma_1+\coth(kh_2)\sigma_2\right\}+\\ +2k^3\left[\rho_1\nu_1U_1\coth(kh_1)+\rho_2\nu_2U_2\coth(kh_2)\right].\end{gathered}\tag{11}$$

To analyze equation (11) while considering the influence of weak acoustic fields, we adopt the approach used in [14; 15]. According to this method:

$$\begin{gathered}a_0\frac{d^2f}{dt^2}+2(a_1+ib_1)\frac{df}{dt}+(a_2+ib_2)f=0;\\ a_2=c-C_{ac}\cos(\Omega t);\quad C_{ac}=(\rho_2-\rho_1)\Omega kU_a;\\ c=-k^2\left[\rho_1U_1^2\coth(kh_1)+\rho_2U_2^2\coth(kh_2)\right]+\gamma k^3+\\ +(\rho_1-\rho_2)gk+\varepsilon_1\varepsilon_0k^2\left[\frac{(\sigma_1-\sigma_2)E_{20x}^2}{\coth(kh_1)\sigma_1+\coth(kh_2)\sigma_2)}-\right.\\ \left.-\frac{\sigma_2^2(\sigma_1-\sigma_2)\coth(kh_1)\coth(kh_2)E_{20z}^2}{\sigma_1^2\left[\coth(kh_1)\sigma_1+\coth(kh_2)\sigma_2\right]}\right]+\\ +\varepsilon_2\varepsilon_0k^2\left[\frac{(\sigma_1-\sigma_2)\coth(kh_1)\coth(kh_2)E_{20z}^2}{\coth(kh_1)\sigma_1+\coth(kh_2)\sigma_2}-\right.\\ \left.-\frac{(\sigma_1-\sigma_2)E_{20x}^2}{\coth(kh_1)\sigma_1+\coth(kh_2)\sigma_2}\right],\end{gathered}\tag{12}$$

where f is a time-dependent function and represents the sum of a "slow" disturbance component $A_1(t) = f_1\exp(\omega t)$, and a "fast" disturbance component, $A_2(t) = f_2\cos(\Omega t)$, which corresponds to acoustic vibrations. Here Ω is the frequency of the acoustic influence [14; 15]. Substituting this sum into equation (7) and discarding the cosine and sine terms, considering that $f_2 = -C_{ac}A_1/(a_0\Omega^2)$ [14], we obtain:

$$a_0\omega^2 + 2(a_1 + ib_1)\omega + c + ib_2 + \frac{C_{ac}^2}{2a_0\Omega^2} = 0. \qquad (13)$$

The solution of equation (7) takes the form:

$$\omega_1 = -\frac{a_1 + ib_1}{a_0} + \frac{\sqrt{(a_1 + ib_1)^2 - a_0\left(c + \frac{C_{ac}^2}{2a_0\Omega^2} + ib_2\right)}}{a_0};$$
$$\omega_2 = -\frac{a_1 + ib_1}{a_0} - \frac{\sqrt{(a_1 + ib_1)^2 - a_0\left(c + \frac{C_{ac}^2}{2a_0\Omega^2} + ib_2\right)}}{a_0}. \qquad (14)$$

The second root of equation (8) has no physical significance and is therefore not considered. The growth rate of disturbances at the liquid interface is determined as $\alpha = \mathrm{Re}(\omega_1)$. Consequently, we obtain:

$$\alpha = -\frac{a_1}{a_0} + \frac{1}{2a_0}\left[2\left(a_1^2 + b_1^2 - a_0\right) - \frac{C_{ac}^2}{\Omega^2} + 2\sqrt{\left(a_1^2 + b_1^2 - a_0c - \frac{C_{ac}^2}{2\Omega^2}\right)^2 + (2a_1b_1 - b_2a_0)^2}\right]^{1/2}. \qquad (15)$$

The data for calculations using equation (9) are presented in the Table.

Research results and discussion

Air-water system

In Fig. 2, *a*, the dependencies of the growth rate of disturbances at the air–water interface on the wavenumber in the absence of an acoustic field under the influence of electric fields are shown. The velocity difference between the horizontal layers was 15 m/s. This function has only one maximum, regardless of the presence of an electric field (curves *1* – *3*). A tangential electric field (β = 0) with a strength of approximately $3\cdot10^6$ V/m stabilizes the Kelvin–Helmholtz instability, which is expressed in a decrease in α_m and a shift of the maximum mode k_m toward lower values (curve *2*). A normal electric field (β = π/2) of the same strength, on the contrary, enhances this instability (curve *3*), which is consistent with widely accepted concepts [8; 19]. At inclination angles of the electric field vector β π/6, π/4, π/3 (Fig. 2, *b*), an increase in k_m is observed from 59,170 m^{-1} (λ_m = 106.19 μm) at β = π/6 to 119,709 m^{-1} (λ_m = 52.48 μm) at β = π/3. The analysis of neutral curves (Fig. 2, *c*) showed that the presence of a vertical component of the electric field significantly narrows the range of relative velocity differences between the fluids, within which capillary forces and the tangential electric field suppress the Kelvin–Helmholtz instability. It should be noted that a similar effect was observed in [8] for the case of inviscid dielectric liquids.

Let us consider the combined influence of weak acoustic and inclined electric fields on the Kelvin–Helmholtz instability. Fig. 3, *a* shows the dependencies of the disturbance growth rate at an amplitude value of the acoustic oscillation velocity U_a = 5 m/s. These dependencies indicate that acoustic vibrations suppress the Kelvin–Helm-

Characteristics of the materials and parameters of external influence

Характеристики материалов и параметры внешнего воздействия

Characteristic	Characteristic values			
	Water	Air	Iron	Argon
Density, kg/m^3	997	1.1308	6700	0.2434
Viscosity, μ, Pa·s	$8.94\cdot10^{-4}$	$1.7798\cdot10^{-5}$	$4.4\cdot10^{-3}$	$8.07\cdot10^{-5}$
Surface tension, σ, N/m	0.059		1.2	
Specific electrical conductivity, S/m	0.01	0.001	$7.52\cdot10^5$	10^3
Dielectric permittivity	81	1	4640	1
Velocity of the first fluid, U_1, m/s	1	–	1	–
Velocity of the second fluid, U_2, m/s	–	16	–	101
Thickness of the first fluid, h_1, m	10^{-3}	10^{-3}	10^{-3}	10^{-3}
Thickness of the second fluid, h_2, m	$3\cdot10^{-3}$	$3\cdot10^{-3}$	$3\cdot10^{-3}$	$3\cdot10^{-3}$

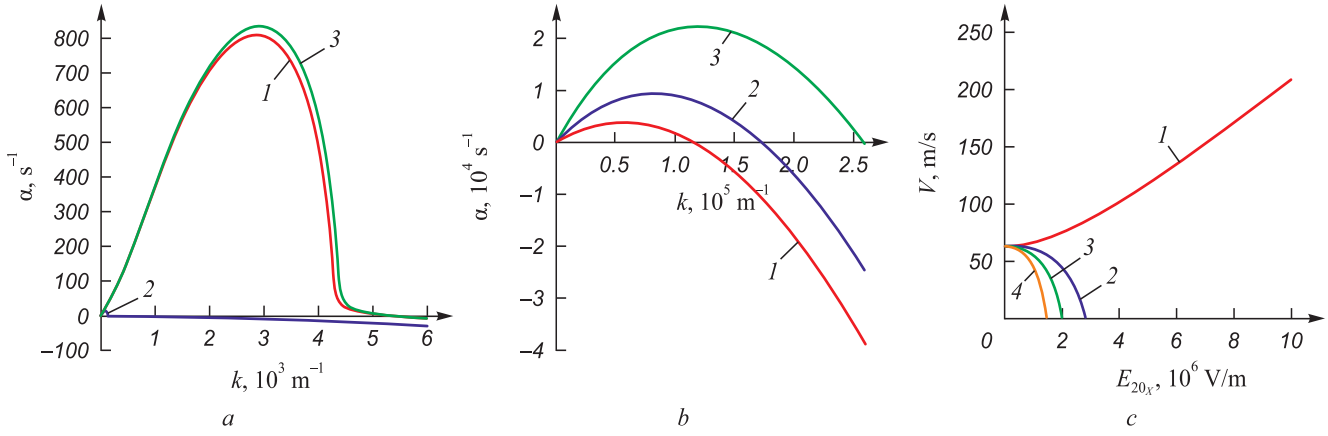

Fig. 2. Dependences of growth rate of perturbations of the air–water interface (*a*, *b*) and neutral curves (*c*) under the influence of electric fields (notation here and in Fig. 3):
a: *1* – without field action; *2* – at $E_{20x} = 3 \cdot 10^6$ V/m and $E_{20z} = 0$ V/m; *3* – at $E_{20x} = 0$ V/m and $E_{20z} = 3 \cdot 10^6$ V/m;
b: *1 – 3* – angle of inclination of the electric field π/6, π/4, and π/3, respectively;
c: *1 – 4* – angle of inclination of the electric field π/6, π/4, and π/3, respectively

Рис. 2. Зависимости скорости роста возмущений поверхности раздела воздух – вода (*a*, *b*) и нейтральные кривые (*c*) при воздействии электрических полей (обозначения здесь и на рис. 3):
a: *1* – без воздействия поля; *2* – при $E_{20x} = 3 \cdot 10^6$ В/м и $E_{20z} = 0$ В/м; *3* – при $E_{20x} = 0$ В/м и $E_{20z} = 3 \cdot 10^6$ В/м;
b: *1 – 3* – угол наклона электрического поля π/6, π/4 и π/3 соответственно;
c: *1 – 4* – угол наклона электрического поля 0, π/6, π/4 и π/3 соответственно

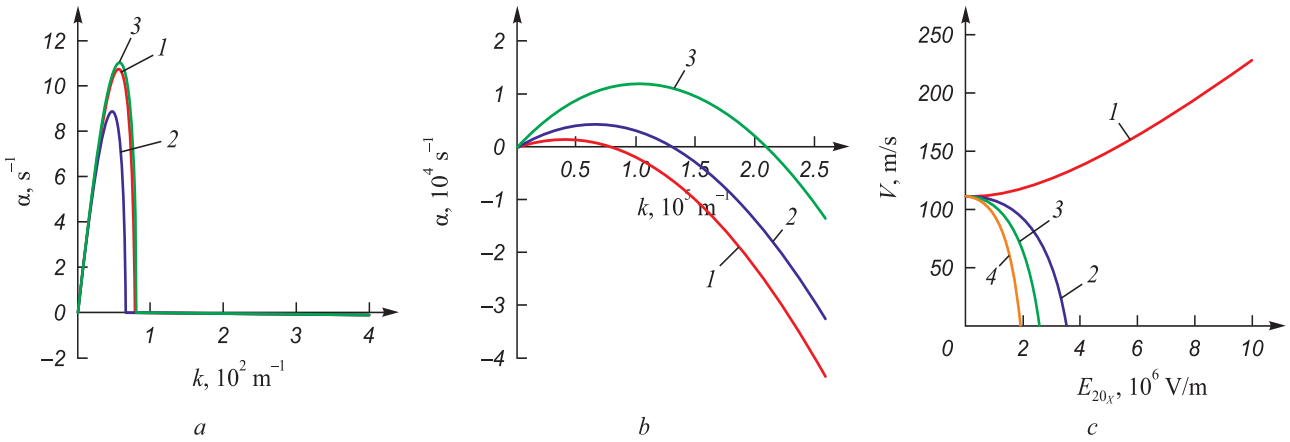

Fig. 3. Dependences of the growth rate of disturbances of the air–water interface (*a*, *b*) and neutral curves (*c*) under the combined action of electric fields and acoustic vibrations with a velocity amplitude of 5 m/s

Рис. 3. Зависимости скорости роста возмущений поверхности раздела воздух–вода (*a*, *b*) и нейтральные кривые (*c*) при совместном воздействии электрических полей и акустических колебаний с амплитудой скорости 5 м/с

holtz instability (curves *1 – 3*), with the tangential electric field amplifying this effect (curve *2*), while the normal electric field, on the contrary, weakens it. A weakening of the suppression effect is also observed at electric field inclination angles β π/6, π/4, π/3 (Fig. 3, *b*), which is confirmed by the analysis of neutral curves (Fig. 3, *c*). Notably, similar suppression phenomena of the Kelvin–Helmholtz instability were identified in [14]. However, in that study, the application of acoustic fields resulted in a rightward shift of k_m, while the maximum growth rate increased, indicating an enhancement of the Kelvin–Helmholtz instability. The discrepancy between the results of [14] and the present study may be explained by the fact that in [14], the ratio $\frac{C_{ac}^2}{2a_0\Omega^2}$ in equation (8) was taken with a negative sign, whereas in this study, it was taken with a positive sign.

Argon-iron system

Now, let us consider a different situation that arises in surfacing or welding processes. In these processes, when the electrode melts in an argon shielding gas environment, a jet of liquid metal forms, which, under certain conditions, breaks up into droplets [20]. The mode of material transfer determines the quality of the formed coating,

making the development of methods for controlling this process an important task. In this system, the mutual flow of gas and liquid gives rise to the Kelvin–Helmholtz instability [20]. Fig. 4, *a* presents dispersion curves, showing that they exhibit two maxima. According to [13], the first maximum is hydrodynamic, while the second is viscosity-induced (curve *1*). The application of a tangential electric field with a strength of $3 \cdot 10^7$ V/m leads to the near-complete suppression of the hydrodynamic maximum (curve *2*), whereas in a normal electric field, this effect is weaker (curve *3*). As results of [19] show, the change in the sign of the influence of the transverse electric field on capillary instability is associated with the ratio of the specific electrical conductivities $\sigma = \sigma_2/\sigma_1$ and the dielectric permittivities of the fluids $\varepsilon = \varepsilon_2/\varepsilon_1$. If $\varepsilon > \sigma$, the electric field has a stabilizing effect; otherwise, when ($\varepsilon < \sigma$) the electric field has a destabilizing effect [19]. In the case under consideration (see Table), for the argon–iron system $\sigma \sim 0.00133$, and $\varepsilon \sim 0.0002$, which should indicate a destabilizing effect of the normal field. However, this is not observed (Fig. 4, *a*). This discrepancy with capillary instability can be explained by the fact that, in this case, the relative velocity of the flowing layers becomes significant, altering the condition for the occurrence of Kelvin–Helmholtz instability maxima [21]. A further increase in the specific electrical conductivity ratio σ beyond 0.012 leads to the restoration of the hydrodynamic maximum and the complete suppression of the viscosity-induced

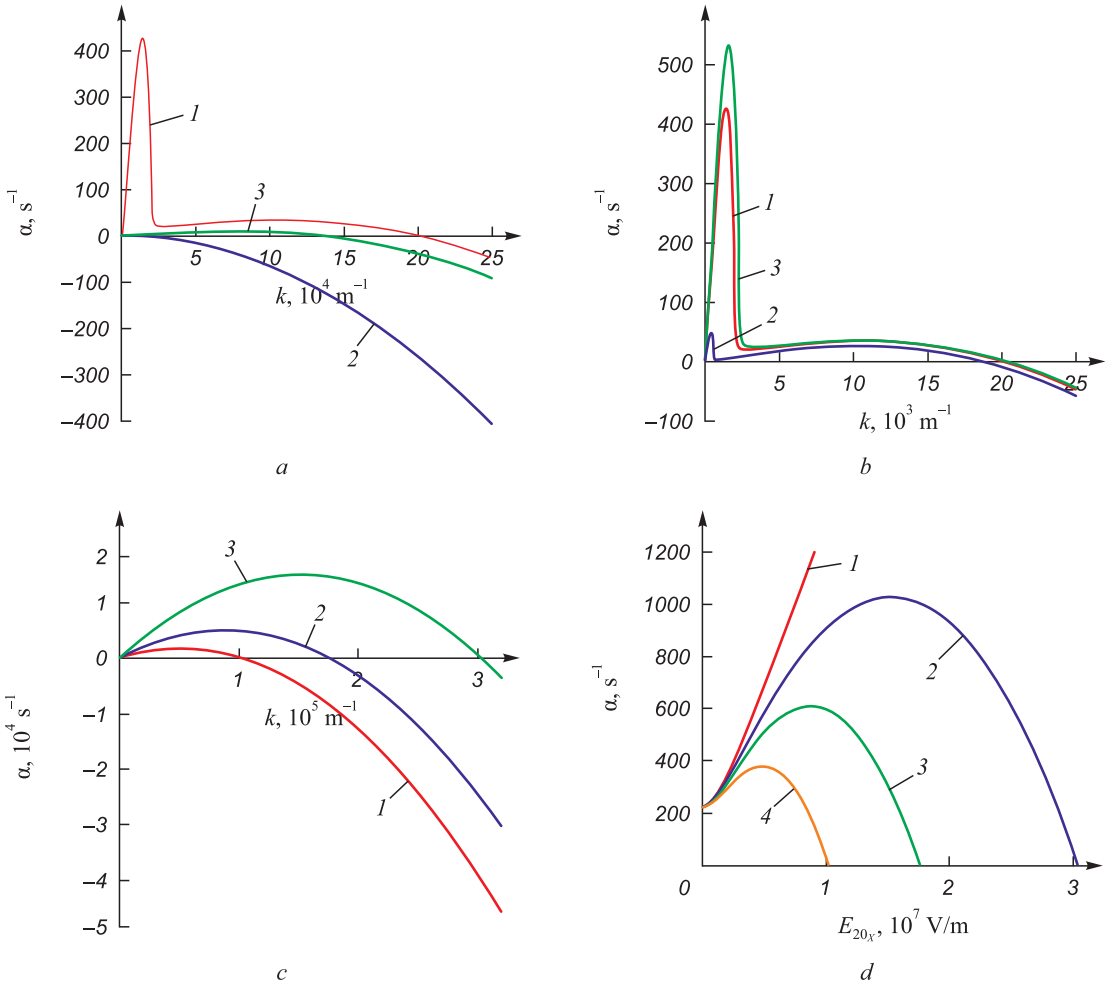

Fig. 4. Dependences of the growth rate of disturbances of the argon–iron interface (*a* – *c*) and neutral curves (*d*) under the combined action of electric fields (notation here and in Fig. 5):
a: *1* – without field action; *2* – at $E_{20x} = 3 \cdot 10^7$ V/m and $E_{20z} = 0$ V/m; *3* – at $E_{20x} = 0$ В/м V/m and $E_{20z} = 3 \cdot 10^7$ V/m;
b: *1* – *3* – angle of inclination of the electric field π/6, π/4, and π/3, respectively;
c: at σ ≥ 0.012: *1* – without field action; *2* – at $E_{20z} = 3 \cdot 10^7$ V/m and σ = 0.013, $E_{20x} = 0$ V/m; *3* – at $E_{20z} = 3 \cdot 10^7$ V/m and σ = 0.015, $E_{20x} = 0$ V/m;
d: *1* – *4* – angle of inclination of the electric field 0, π/6, π/4 and π/3, respectively

Рис. 4. Зависимости скорости роста возмущений поверхности раздела аргон–железо (*a* – *c*) и нейтральные кривые (*d*) при совместном воздействии электрических полей (обозначения здесь и на рис. 5):
a: *1* – без воздействия поля; *2* – при $E_{20x} = 3 \cdot 10^7$ В/м и $E_{20z} = 0$ В/м; *3* – при $E_{20x} = 0$ В/м и $E_{20z} = 3 \cdot 10^7$ В/м;
b: *1* – *3* – угол наклона электрического поля π/6, π/4 и π/3 соответственно;
c: при σ ≥ 0,012: *1* – без воздействия поля; *2* – при $E_{20z} = 3 \cdot 10^7$ В/м и σ = 0,013, $E_{20x} = 0$ В/м; *3* – при $E_{20z} = 3 \cdot 10^7$ В/м и σ = 0,015, $E_{20x} = 0$ В/м;
d: *1* – *4* – угол наклона электрического поля 0, π/6, π/4 и π/3 соответственно

maximum. When $\sigma \geq 0.015$, the effect changes from stabilizing to destabilizing (Fig. 4, *b*). The results of studying the effect of inclined electric fields (Fig. 4, *c*) showed that these fields enhance the Kelvin–Helmholtz instability regardless of the values of σ and ε. In this case, the maximum growth rate is viscosity-induced. At field strengths $E_{20x} < 3 \cdot 10^7$ V/m, a weakly pronounced hydrodynamic maximum is observed. The neutral stability curves indicate that, as in the air–water system, a reduction in the stability region of interface disturbances is observed (Fig. 4, *d*).

The combined effect of acoustic vibrations with a velocity amplitude of 10 m/s and an electric field with a strength of $3 \cdot 10^7$ /V/m at $\sigma \sim 0.00133$, and $\varepsilon \sim 0.0002$, on the contrary, leads to the complete suppression of the viscosity-induced instability maximum (Fig. 5, *a*, curve *1*) and a sharp reduction in the maximum growth rate α_m of disturbances of hydrodynamic origin. The application of a horizontal electric field significantly weakens this effect (Fig. 5, *a*, curve *2*), while in a vertical field, this effect, on the contrary, is amplified (Fig. 5, *a*, curve *3*), despite the fact that at $E_{20x} = 0$ and $E_{20z} = 3 \cdot 10^7$ V/m, the value of k_m is greater than $E_{20x} = 3 \cdot 10^7$ V/m and $E_{20z} = 0$. A change in the sign of the effect to destabilizing also occurs at $\sigma \geq 0.015$ (Fig. 5, *b*). The application of an inclined electric field, as in the absence of sound, enhances the Kelvin–Helmholtz instability, but α_m is somewhat lower (Fig. 5, *c*). The neutral curves (Fig. 5, *d*) show an increase in the range of fluid velocities in which capillary forces and tangential fields suppress the Kelvin–Helmholtz instability under the influence of an acoustic field.

Conclusions

Inclined electric fields contribute to the enhancement of the Kelvin–Helmholtz instability at the interfaces of conducting fluids, regardless of the ratio of their den-

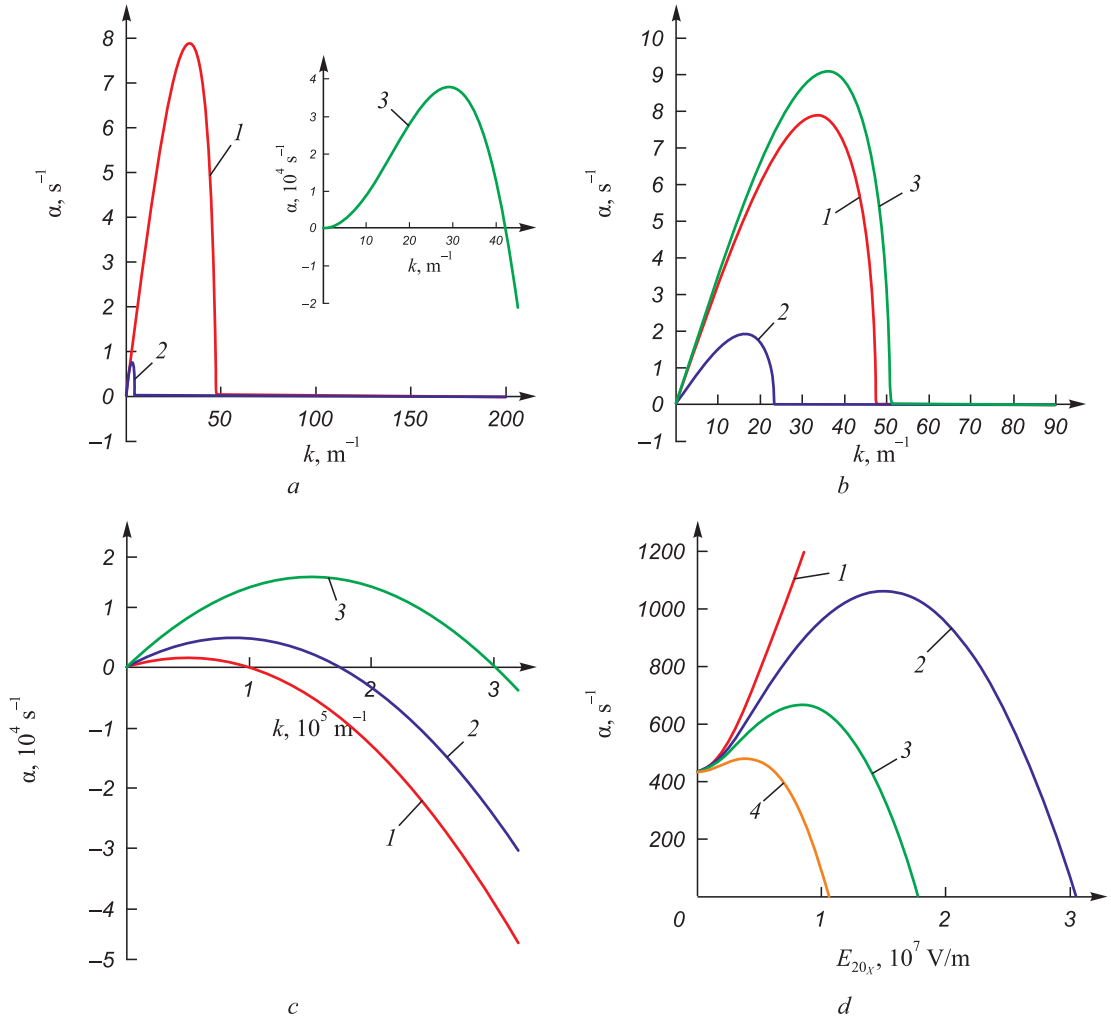

Fig. 5. Dependences of the growth rate of disturbances of the argon – iron interface (*a* – *c*) and neutral curves (*d*) under the combined action of electric fields and acoustic vibrations with a velocity amplitude of 10 m/s

Рис. 5. Зависимости скорости роста возмущений поверхности раздела аргон – железо (*a* – *c*) и нейтральные кривые (*d*) при совместном воздействии электрических полей и акустических колебаний с амплитудой скорости 10 м/с

sities, specific electrical conductivities, and the presence of acoustic fields.

It has been established that the combined application of inclined electric fields and acoustic vibrations in the air – water system allows the formation of liquid droplets in the range of 10 to 100 μm, even at low gas flow velocities. This opens up new prospects for the development of accelerated cooling technologies for rolled products to achieve high hardness and impact toughness.

For the argon–iron system, it has been shown that a vertical electric field at $\sigma \sim 10^{-3}$ and $\varepsilon \sim 10^{-4}$ practically suppresses the hydrodynamic maximum. An increase in the specific electrical conductivity ratio σ beyond 0.012, on the contrary, leads to the restoration of the hydrodynamic maximum and the complete suppression of the viscosity-induced one. At $\sigma \geq 0.015$, the effect changes from stabilizing to destabilizing, regardless of the number of maxima in the dependence of the growth rate on the wavelength. The application of a tangential electric field completely suppresses the Kelvin–Helmholtz instability.

The combined effect of acoustic vibrations and a normal electric field leads to the complete suppression of the viscosity-induced instability maximum and a sharp reduction in the maximum growth rate of disturbances of hydrodynamic origin, while in a horizontal electric field, this effect is significantly weaker.

References / Список литературы

1. Praturi D.S., Girimaji S.S. Mechanisms of canonical Kelvin-Helmholtz instability suppression in magnetohydrodynamic flows. *Physics of Fluids*. 2019;31(2):024108. https://doi.org/10.1063/1.5083857
2. Rahmani M., Seymour B.R., Lawrence G.A. The effect of Prandtl number on mixing in low Reynolds number Kelvin-Helmholtz billows. *Physics of Fluids*. 2016;28(5):054107. https://doi.org/10.1063/1.4949267
3. Panin V.E., Gromov V.E., Romanov D.A., Budovskikh E.A., Panin S.V. The physical basics of structure formation in electroexplosive coatings. *Doklady Physics*. 2017;62:67–70. https://doi.org/10.1134/S1028335817020112
4. Mishin V.V., Tomozov V.M. Kelvin–Helmholtz instability in the solar atmosphere, solar wind and geomagnetosphere. *Solar Physics*. 2016;291:3165–3184. https://doi.org/10.1007/s11207-016-0891-4
5. Petrarolo A., Kobald M., Schlechtriem S. Understanding Kelvin–Helmholtz instability in paraffin-based hybrid rocket fuels. *Experiments in Fluids*. 2018;59:62. https://doi.org/10.1007/s00348-018-2516-1
6. Grigor'ev A.I., Shiryaev A.A., Shiryaeva S.O. Instability of a charged droplet in an inhomogeneous electrostatic field of a rod of finite thickness. *Fluid Dynamics*. 2018;53(1):34–48. https://doi.org/10.1134/S0015462818010081

   Григорьев А.И., Ширяев А.А., Ширяева С.О. Неустойчивость заряженной капли в неоднородном электростатическом поле стержня конечной толщины. *Известия РАН. Механика жидкости и газа*. 2018;(1):36–50. https://doi.org/10.7868/S0568528118010048
7. Saraev Yu.N., Chinakhov D.A., Ilyashchenko D.I., Kiselev A.S., Gordynets A.S. Investigation of the stability of melting and electrode metal transfer in consumable electrode arc welding using power sources with different dynamic characteristics. *Welding International*. 2017;31(10):784–790. https://doi.org/10.1080/09507116.2017.1343977
8. Korovin V.M. Effect of tilted electrostatic field on the Kelvin–Helmholtz instability in a liquid dielectric and gas flow. *Technical Physics*. 2017;62:1316–321. https://doi.org/10.1134/S1063784217090134
9. Sarychev V.D., Khaimzon B.B., Nevskii S.A., Il'yashchenko A.V., Grishunin V.A. Mathematical models of mechanisms for rolled products accelerated cooling. *Izvestiya. Ferrous Metallurgy*. 2018;61(4):326–332. (In Russ.). https://doi.org/10.17073/0368-0797-2018-4-326-332

   Сарычев В.Д., Хаимзон Б.Б., Невский С.А., Ильященко А.В., Гришунин В.А. Математические модели механизмов ускоренного охлаждения проката. *Известия вузов. Черная металлургия*. 2018;61(4):326–332. https://doi.org/10.17073/0368-0797-2018-4-326-332
10. Awasthi M.K., Asthana R., Agrawal G.S. Viscous correction for the viscous potential flow analysis of Kelvin–Helmholtz instability of cylindrical flow with heat and mass transfer. *International Journal of Heat and Mass Trans*. 2014;78:251–259. https://doi.org/10.1016/j.ijheatmasstransfer.2014.06.082
11. Barreras F., Lozano A., Dopazo C. Linear instability analysis of the viscous longitudinal perturbation on an air-blasted liquid sheet. *Atomization and Sprays*. 2001;11(2):139–154. https://doi.org/10.1615/ATOMIZSPR.V11.I2.30
12. Logvinov O.A. Linear stability of stratified flow of two viscous fluids. *Moscow University Mechanics Bulletin*. 2022;77; 117–126. https://doi.org/10.3103/S0027133022040021
13. Sarychev V.D., Granovskii A.Yu., Gromov V.E. Model of formation of inner nanolayers in shear flows of material. *Technical Physics*. 2013;58(10):1544–157. https://doi.org/10.1134/S1063784213100113
14. Bychkov V. Analytical scalings for flame interaction with sound waves. *Physics of Fluids*. 1999;11(10):3168–3173. https://doi.org/10.1063/1.870173
15. Bilgili S., Ugarte O., Akkerman V. Interplay of Kelvin–Helmholtz instability with acoustics in a viscous potential flow. *Physics of Fluids*. 2020;32(8):084108. https://doi.org/10.1063/5.0017448
16. Awasthi M.K., Dutt N., Kumar A., Kumar S. Electrohydrodynamic capillary instability of Rivlin–Ericksen viscoelastic fluid film with mass and heat transfer. *Heat Transfer*. 2024;53(1):115–133. https://doi.org/10.1002/htj.22944
17. Saville D.A. Electrohydrodynamic stability: effects of charge relaxation at the interface of a liquid jet. *Journal of Fluid Mechanics*. 1971;48(4):815–827. https://doi.org/10.1017/S0022112071001873
18. Shkadov V.Ya., Shutov A.A. Stability of a surface-charged viscous jet in an electric field. *Fluid Dynamics*. 1998;33(2):176–185. https://doi.org/10.1007/BF02698699
19. Awasthi M.K. Study on electrohydrodynamic capillary instability of viscoelastic fluids with radial electric field. *Inter-*

national Journal of Applied Mechanics. 2014;6(4):1450037. https://doi.org/10.1142/S1758825114500379

20. Zhao Y., Chung H. Numerical simulation of droplet transfer behavior in variable polarity gas metal arc welding. *International Journal of Heat and Mass Transfer*. 2017;111:1129–1141. https://doi.org/10.1016/j.ijheatmasstransfer.2017.04.090

21. Nevskii S.A., Sarychev V.D., Granovsky A.Yu., Bashchenko L.P., Gromov V.E. Formation of micro- and nano- in electroexplosive carboborization of titanium alloys by the mechanism hydrodynamic instabilities. *Fundamental'nye problemy sovremennogo materialovedenia (Basic Problems of Material Science (BPMS))*. 2023;20(3):317–328. (In Russ.). https://doi.org/10.25712/ASTU.1811-1416.2023.03.004

Невский С.А., Сарычев В.Д., Грановский А.Ю., Бащенко Л.П., Громов В.Е. Формирование микро- и наноструктур при электровзрывном карбоборировании титановых сплавов по механизму гидродинамических неустойчивостей. *Фундаментальные проблемы современного материаловедения*. 2023;20(3):317–328. https://doi.org/10.25712/ASTU.1811-1416.2023.03.004

Information about the Authors / Сведения об авторах

Sergei A. Nevskii, *Dr. Sci. (Eng.), Assist. Prof. of the Chair of Science named after V.M. Finkel'*, Siberian State Industrial University
ORCID: 0000-0001-7032-9029
E-mail: nevskiy_sa@physics.sibsiu.ru

Lyudmila P. Bashchenko, *Cand. Sci. (Eng.), Assist. Prof. of the Chair "Thermal Power and Ecology"*, Siberian State Industrial University
ORCID: 0000-0003-1878-909X
E-mail: luda.baschenko@gmail.com

Vladimir D. Sarychev, *Cand. Sci. (Eng.), Assist. Prof. of the Chair of Sciences named after V.M. Finkel'*, Siberian State Industrial University
ORCID: 0000-0002-4861-0778
E-mail: sarychev_vd@mail.ru

Aleksei Yu. Granovskii, *Cand. Sci. (Eng.), Senior Researcher of the Department of Scientific Research*, Siberian State Industrial University
ORCID: 0009-0006-4583-8431
E-mail: legatokun@gmail.com

Diana V. Shamsutdinova, *Student of Institute of Pedagogical Education*, Siberian State Industrial University
E-mail: dianas1009hamsutdinova@gmail.com

Сергей Андреевич Невский, *д.т.н., доцент кафедры естественнонаучных дисциплин им. профессора В.М. Финкеля*, Сибирский государственный индустриальный университет
ORCID: 0000-0001-7032-9029
E-mail: nevskiy_sa@physics.sibsiu.ru

Людмила Петровна Бащенко, *к.т.н., доцент кафедры теплоэнергетики и экологии*, Сибирский государственный индустриальный университет
ORCID: 0000-0003-1878-909X
E-mail: luda.baschenko@gmail.com

Владимир Дмитриевич Сарычев, *к.т.н., доцент кафедры естественнонаучных дисциплин им. профессора В.М. Финкеля*, Сибирский государственный индустриальный университет
ORCID: 0000-0002-4861-0778
E-mail: sarychev_vd@mail.ru

Алексей Юрьевич Грановский, *к.т.н., старший научный сотрудник Управления научных исследований*, Сибирский государственный индустриальный университет
ORCID: 0009-0006-4583-8431
E-mail: legatokun@gmail.com

Диана Витальевна Шамсутдинова, *студент Института педагогического образования*, Сибирский государственный индустриальный университет
E-mail: dianas1009hamsutdinova@gmail.com

Contribution of the Authors / Вклад авторов

S. A. Nevskii – problem statement, obtaining and analyzing the dispersion equation, discussion and verification of modeling results.

L. P. Baschenko – calculations, discussion of results, design of the article.
V. D. Sarychev – formulation of the work idea, analysis and discussion of research results, verification of modeling results.
A. Yu. Granovskii – analysis and discussion of research results, verification.
D. V. Shamsutdinova – discussion of results, analysis of literary sources on the Kelvin–Helmholtz instability.

С. А. Невский – постановка задачи, получение и анализ дисперсионного уравнения, обсуждение и верификация результатов моделирования.
Л. П. Бащенко – проведение расчетов, обсуждение результатов, оформление статьи.
В. Д. Сарычев – идея работы, анализ и обсуждение результатов исследования, верификация результатов моделирования.
А. Ю. Грановский – анализ и обсуждение результатов исследования, верификация результатов моделирования.
Д. В. Шамсутдинова – обсуждение результатов, анализ литературных источников по неустойчивости Кельвина–Гельмгольца.

Received 09.04.2024
Revised 09.06.2024
Accepted 17.12.2024

Поступила в редакцию 09.04.2024
После доработки 09.06.2024
Принята к публикации 17.12.2024